A LETTERS JOURNAL EXPLORING THE FRONTIERS OF PHYSICS

LETTER

Fluctuations of entropy production in partially masked electric circuits

To cite this article: Kuan-Hsun Chiang *et al* 2016 *EPL* **113** 30001

A Letters Journal Exploring the Frontiers of Physics

February 2016

EPL, **113** (2016) 30001 www.epljournal.org
doi: 10.1209/0295-5075/113/30001

Fluctuations of entropy production in partially masked electric circuits

Kuan-Hsun Chiang, Chia-Wei Chou, Chi-Lun Lee[(a)], Pik-Yin Lai and Yung-Fu Chen[(b)]

Department of Physics, National Central University - Jhongli 32001, Taiwan

received 10 November 2015; accepted in final form 9 February 2016
published online 23 February 2016

PACS 05.40.-a – Fluctuation phenomena, random processes, noise, and Brownian motion
PACS 05.70.Ln – Nonequilibrium and irreversible thermodynamics

Abstract – We experimentally investigate fluctuations of entropy production in a coupled driven-RC circuit. In particular, we focus on the hidden-variable problem, where part of the circuit is neglected intentionally. In the two versions of the reduced descriptions we provide for the system, the fluctuation theorem (FT) is valid in all timescales for weak coupling. However, FT fails in the strong-coupling regime, in the short-time limit for one version, and in the long-time limit for the other. In these timescales where FT fails, both descriptions still give FT-like behavior. The failure of FT implies non-Markovian dynamics, meaning there exists a hidden variable that cannot be incorporated into the heat bath. We argue that FT can be restored with the introduction of a timescale-dependent effective noise.

Introduction. – In the studies of statistical mechanical systems, it is often necessary to analyze the behavior of a microscopic or mesoscopic object which is assumed to be thermalized by a heat reservoir. Simple examples are Brownian motions of colloids and relaxation dynamics of polymers. The object of interest keeps exchanging energy with its environment, which facilitates dynamic or configurational transitions. Despite the success often achieved via such scenarios, one is still tempted to ask: under what circumstances would this heat-bath assumption become invalid? In particular, if the surrounding bath consists of entities which are scalewise similar to the subject of interest, could the exchanged energy simply be regarded as heat? The answer lies in how one classifies the interactions within the system-surroundings dynamics into fast and slow modes, or equivalently, effective behaviors in Markovian and non-Markovian regimes.

In this work we consider a simple example, *i.e.*, a network of two resistor-capacitor (RC) circuits (see fig. 1(a)). The interaction between the two RC circuits is introduced through a coupling capacitor, and thermal fluctuations are presented through Johnson-Nyquist noises on both resistors. Our aim is to explore the role of the second RC circuit, especially when it can be regarded as part of the heat bath. For this network we investigate its thermal-equilibrium and- non-equilibrium steady states (NESS), the latter providing hints for the statistical mechanics of driven particles. Specifically, for both the complete and reduced descriptions of the network, we examine experimentally the fluctuation theorem (FT) [1,2], whose validity, if exists, states that the entropy production distribution should follow the relation $P(\Delta S_{\text{tot}} = +a)/P(\Delta S_{\text{tot}} = -a) = \exp(a/k_B)$, where k_B is Boltzmann's constant.

The entropy production inferred from a reduced description, namely, the apparent entropy [3,4], is derived from measurements with incomplete information, and may be distinct from the real entropy production. Theoretically, the characteristics of apparent entropy have been studied extensively. For example, FT was verified by a system with coarse-grained description [5] or partially masked dynamics [6]; the excessive part of entropy production in NESS was reported to be invariant over descriptions of different timescales [7]; the relation between the hidden entropy production and fast variables was discussed in a harmonic system of two coupled Brownian particles [8]; a simulated work performed in coupled two-level systems demonstrated that entropy production based on observing merely one system can deviate from FT [9]. Despite the theoretical progresses, relevant experimental works are very limited. As a pivot example, a system of two magnetically coupled colloidal particles is investigated in ref. [3], where the role of the masked slow variables is

(a) E-mail: chilun@ncu.edu.tw
(b) E-mail: yfuchen@cc.ncu.edu.tw

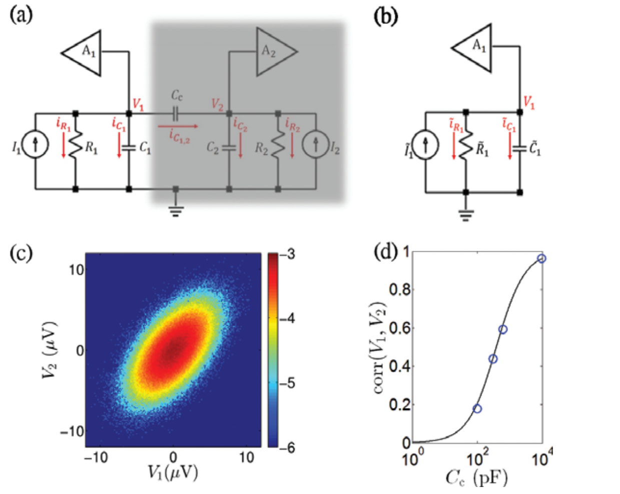

Fig. 1: (Colour online) (a) Diagram of the coupled-RC system. The signals V_1 and V_2 are extracted by low-noise amplifiers A_1 and A_2. The values $R_1 = 9.10\,\mathrm{M\Omega}$, $C_1 = 429\,\mathrm{pF}$, and $R_2 = 9.18\,\mathrm{M\Omega}$, $C_2 = 352\,\mathrm{pF}$ are derived experimentally via the power spectra of isolated RC circuits. Various values of C_c are used in our study. The circuit can be driven away from thermal equilibrium via constant injected currents. (b) Masked description. The shadowed part of (a) and the signal V_2 are neglected intentionally. Note that the reduced parameters ($\tilde{R}_1$, $\tilde{C}_1$, and $\tilde{I}_1$) can be different from the original ones. (c) Joint probability $\log P_{\mathrm{ss}}(V_1, V_2)$ with $C_c = 620\,\mathrm{pF}$ and $I_1 = I_2 = 0$. (d) Measured correlation coefficient of V_1 and V_2 *vs.* C_c. The value of C_c is measured by a LCR meter. The solid curve shows the theoretical prediction by ref. [15].

addressed. The apparent entropy production was found to follow a FT-like behavior. Nevertheless, the form of coupling is complicated, and further mathematical analysis lacks therein.

The electric circuit can serve as one of the simplest templates in the studies of small-scale non-equilibrium thermodynamics [10,11]. In a single-RC circuit, FT is satisfied if heat and Shannon entropy are both considered in the total entropy production [12]. In ref. [13], NESS of a coupled-RC system were studied where a net heat flow exists due to the temperature difference between the resistors. Furthermore, a quantum version of heat exchange between two coupled resistors owing to photon scattering was investigated theoretically [14].

In the present work, we investigate the hidden-variable problem via the consideration of a simple coupled network of two RC circuits, where the coupling form is well understood. As the corresponding coupled stochastic equations are linear, theoretical analysis can be applied using the fluctuation-dissipation theorem (FDT) and compared with our experimental observations.

Experimental setup. – Figure 1(a) illustrates our experimental system. Two RC circuits R_1C_1 and R_2C_2, with driven currents I_1 and I_2, are coupled through a capacitor C_c of varying strength. The resistors and capacitors have nominal values $R_1 = R_2 = 10.0\,\mathrm{M\Omega}$ and $C_1 = C_2 = 300\,\mathrm{pF}$, respectively, and these elements remain unchanged throughout our study. The experiments are performed at room temperature $T = 298\,\mathrm{K}$. For each experimental run, we record time traces of 5×10^5 timesteps for the voltages V_1 and V_2 across R_1 and R_2, respectively, with a sampling rate of 1024 Hz. The exact values of the electric elements are determined from fitting the measured power spectral densities of the voltage time series $V_1(t)$ and $V_2(t)$, done at $C_c = 0$, to Lorentzian functions as suggested by FDT [11]. Relevant physical quantities, such as injected power, dissipation heat, and entropy production, are derived subsequently using the voltage time series.

The coupling capacitance C_c introduces a positive correlation between V_1 and V_2, which can be visualized through the steady-state joint probability distribution $P_{\mathrm{ss}}(V_1, V_2)$ in fig. 1(c) (for the case of $C_c = 620\,\mathrm{pF}$). Quantitatively, we can study the correlation using the correlation coefficient $\mathrm{corr}(V_1, V_2)$, which is the normalized covariance between the voltages such that $\mathrm{corr}(V_1, V_2) = 1$ for the maximal correlated case. Figure 1(d) shows that the correlation increases with C_c, as the experimental data agree well with the prediction from FDT (solid line). In the masked circuit, this correlation hints that the energy exchange with the second RC circuit does not merely serve as a background thermal noise, and its contribution can alter the validity of FT under reduced descriptions.

Entropy production evaluated from the complete description. – We first consider the entropy production of the entire circuit. The total entropy production from time t to $t + \tau$ is $\Delta S_{\mathrm{tot},\tau} = \Delta S_{Q,\tau} + \Delta S_{\mathrm{Sh},\tau}$, where $\Delta S_{Q,\tau} = \frac{1}{T}\int_t^{t+\tau}(V_1 i_{R1} + V_2 i_{R2})\,\mathrm{d}t'$ is the entropy production due to the net heat dissipation, and $\Delta S_{\mathrm{Sh},\tau} = -k_B \ln \frac{P_{\mathrm{ss}}(V_1(t+\tau),V_2(t+\tau))}{P_{\mathrm{ss}}(V_1(t),V_2(t))}$ is the change in Shannon entropy. Experimentally, the currents through the resistors i_{R1} and i_{R2} can be derived utilizing Kirchoff's law, as the currents through capacitors can be obtained from the time derivatives of V_1 and V_2. Note that under the complete description, the net heat dissipation used here is identical to the dissipation function derived utilizing the ratio of forward– and time-reversed–transition probabilities in the FDT analysis [15]. Theoretically, one can prove that FT for the complete description holds for all time intervals under NESS.

The thermal-equilibrium result of $\Delta S_{\mathrm{tot},\tau}$ (where $I_1 = I_2 = 0$) shown in fig. 2(a) exhibits a narrow, delta-function–like distribution for all observed values of C_c. It is consistent with the theoretical expectation $\Delta S_{\mathrm{tot},\tau} = 0$ [15] (and hence $\Delta S_{Q,\tau}$ and $\Delta S_{\mathrm{Sh},\tau}$ are perfectly anti-correlated). As a comparison, while the average of $\Delta S_{Q,\tau}$ is zero owing to no injected currents, its corresponding distribution is much broader and non-Gaussian (please refer to the dark-red diamonds in fig. 2(a)). In NESS, where at least one injected current exists, $\Delta S_{Q,\tau}$ and $\Delta S_{\mathrm{Sh},\tau}$ no longer compensate each other perfectly. As a result, $\Delta S_{\mathrm{tot},\tau}$ is broadened into a Gaussian distribution

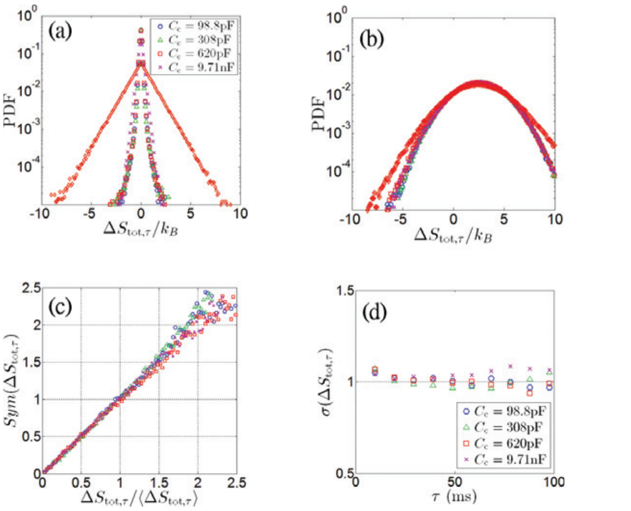

Fig. 2: (Colour online) Entropy production of the circuit with complete information. (a) Equilibrium cases ($I_1 = I_2 = 0$): probability distribution functions $P(\Delta S_{\mathrm{tot},\tau})$ with $\tau = 48.8$ ms and $C_c = 98.8$ pF (blue circles), 308 pF (green triangles), 620 pF (red squares), and 9.71 nF (purple crosses). As a comparison, dark-red diamonds show $P(\Delta S_{Q,\tau})$ for the case $C_c = 620$ pF and $\tau = 48.8$ ms. NESS cases ($I_1 = I_2 = 108$ fA): (b) $P(\Delta S_{\mathrm{tot},\tau})$. (c) Symmetry functions of $\Delta S_{\mathrm{tot},\tau}$ with $\tau = 48.8$ ms. (d) Slopes of symmetry function *vs.* τ. (In (b), (c), and (d) we use the same values of C_c and symbol illustrations as in (a).)

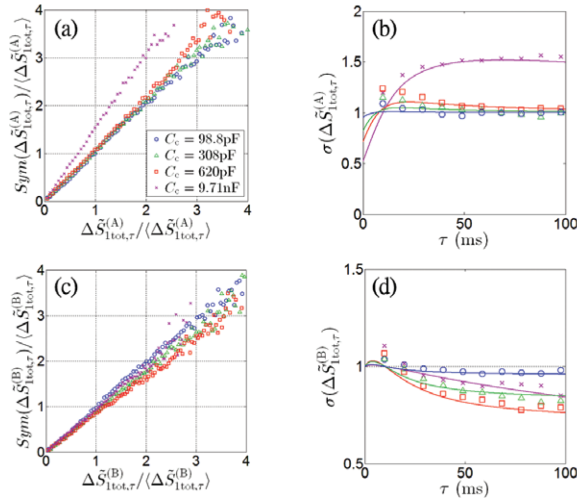

Fig. 3: (Colour online) Entropy production derived from incomplete information. The circuit is driven out of equilibrium by $I_1 = 108$ fA. Naive description (description (A)): (a) symmetry function of $\Delta\tilde{S}^{(A)}_{1\mathrm{tot},\tau}$ with $I_2 = 0$, $C_c = 98.8$ pF (blue circles), 308 pF (green triangles), 620 pF (red squares) and 9.71 nF (purple crosses); $\tau = 48.8$ ms for all data; (b) slope of symmetry function *vs.* τ. Trace-out method (description (B)): (c) symmetry function of $\Delta\tilde{S}^{(B)}_{1\mathrm{tot},\tau}$; (d) corresponding slope in (c) *vs.* τ. (In (b), (c) and (d) we follow the same symbol illustrations as in (a). The solid lines represent theoretical predictions by ref. [15].)

as shown in fig. 2(b). Note that $\langle\Delta S_{\mathrm{tot},\tau}\rangle = \langle\Delta S_{Q,\tau}\rangle = \sum_m I_m^2 R_m \tau/T > 0$ in NESS. To examine the validity of FT, one uses a symmetry function $\mathrm{Sym}(a) \equiv k_B \ln[P(\Delta S_{\mathrm{tot},\tau} = +a)/P(\Delta S_{\mathrm{tot},\tau} = -a)]$. In figs. 2(c) and (d) FT for the complete circuit is demonstrated by the linearity in the symmetry function with slopes close to unity [2].

Entropy production inferred from reduced descriptions. – Experimentally, to derive an effective entropy production $\Delta\tilde{S}_{1\mathrm{tot},\tau}$ from the masked circuit as described in figs. 1(a) and (b), we intentionally ignore the measured time series of V_2, while the measured V_1 is interpreted as that of an effective single-RC circuit. In this work we use two descriptions towards the derivation of effective parameters as well as $\Delta\tilde{S}_{1\mathrm{tot},\tau}$. First we use a naive description (description (A)), where one treats R_2 as a part of the uncorrelated thermal noise and neglect it in the circuit. Thus, we have $\tilde{R}_1 = R_1$, $\tilde{I}_1 = I_1$, and $\tilde{C}_1 = C_1 + C_c C_2/(C_c + C_2)$ is the effective capacitance. The adoption of these effective parameters is supported by the experimental observations in the white-noise level of $V_1(t)$ at low frequencies, $4k_B R_1 T$, and its variance, $k_B T/\tilde{C}_1$. Under this reduced description, the inferred current through $\tilde{R}_1$ is $\tilde{i}_{R1} = \tilde{I}_1 - \tilde{i}_{C1}$, where $\tilde{i}_{C1} = \tilde{C}_1\dot{V}_1$. And the heat dissipation in $\tilde{R}_1$ over time τ is derived as $\tilde{Q}^{(A)}_{1,\tau} = \int_t^{t+\tau} \tilde{i}_{R1} V_1 \mathrm{d}t'$. Therefore, one can define an apparent entropy production [3] $\Delta\tilde{S}^{(A)}_{1\mathrm{tot},\tau} = \tilde{Q}^{(A)}_{1,\tau}/T - k_B \ln[P_{\mathrm{ss}}(V_1(t+\tau))/P_{\mathrm{ss}}(V_1(t))]$.

In thermal equilibrium ($\tilde{I}_1 = 0$), we find again that $\Delta\tilde{S}^{(A)}_{1\mathrm{tot},\tau} = 0$ for all cases, which is supported by our FDT analysis [15]. We next study $\Delta\tilde{S}^{(A)}_{1\mathrm{tot},\tau}$ in NESS (using $\tilde{I}_1 = 108$ fA), where $\langle\Delta\tilde{S}^{(A)}_{1\mathrm{tot},\tau}\rangle = I_1^2 R_1 \tau/T$. As shown in fig. 3(a), most symmetry functions exhibit a linear behavior with slopes close to 1. However, large deviation occurs for $C_c = 9.71$ nF, where the slope is about 1.5. The slopes *vs.* τ are plotted in fig. 3(b), which are in remarkable agreement with our theoretical prediction [15] (solid lines). The slope asymptotically converges to 1 as τ increases, and for smaller C_c the convergence becomes faster. Our result indicates that although $\Delta\tilde{S}^{(A)}_{1\mathrm{tot},\tau}$ is physically distinct from the complete entropy production $\Delta S_{\mathrm{tot},\tau}$, FT in this reduced description is nevertheless obeyed approximately in small-C_c and large-τ regimes.

In addition to the naive description, one can resort to the steady-state ($P_{\mathrm{ss}}(V_1)$) and forward-transition ($P_F(V_1(t+dt)|V_1(t))$) probabilities of V_1 (defined as description (B)). The reduced probabilities can be derived via tracing out the V_2 degree of freedom. We find that these probability distributions are exactly identical to those from an effective single-RC circuit [15], with renormalized elements $\tilde{R}_1 = R_1/\left[1 + \frac{R_1 {C_c}^2}{R_2(C_2+C_c)^2}\right]$, $\tilde{C}_1 = C_1 + \frac{C_c C_2}{C_c + C_2}$, and $\tilde{I}_1 = I_1\left(1 + \frac{R_1 {C_c}^2}{R_2(C_2+C_c)^2}\right)$. Note that R_2 contributes explicitly in this reduced description. On this effective single-RC circuit, the heat dissipating function is $\tilde{Q}^{(B)}_{1,dt} = (-\tilde{C}_1\dot{V}_1 + \tilde{I}_1)V_1\,\mathrm{d}t$. We then evaluate the reduced entropy production $\Delta\tilde{S}^{(\mathrm{B})}_{1\mathrm{tot},\tau}$ using the new heat dissipation function and unmodified Shannon entropy. The resulting symmetry function and its slope are plotted in figs. 3(c) and (d), respectively. We find that for small τ the slope gets considerably closer to 1 for all cases. However, in contrast to description (A), the slope in description (B) deviates from 1 at large τ. The deviation becomes much less prominent at our minimal value of C_c (98.8 pF), while a non-monotonic trend occurs over the increasing of C_c. Again all these features are well captured by the theoretical predictions in ref. [15].

Discussion. – From figs. 3(a) and (c) we find the symmetry functions to be linear in all observed cases with our reduced descriptions. This results from the fact that the total entropies in these reduced descriptions have Gaussian distributions [15]. However, our results indicate that FT in the masked circuit is not strictly obeyed in all our reduced descriptions. The deviation gives a hint that the coupling circuit (R_2C_2) does not simply serve as a background noise, as demonstrated by the voltage correlations in figs. 1(c) and (d). Hence information of the unrecognized circuit can contribute to the characteristics of $V_1(t)$, in contrast with the time trace generated by an ideal single-RC circuit.

To be more specific, the relaxation dynamics of a single-RC circuit is Markovian, in the sense that its transition probability (over time dt) and steady-state distribution suffice to describe the dynamics. Moreover, the complete description of the coupled-RC system fulfills FT, too, owing to the Markovian nature of its full dynamics, which exhibits two intrinsic relaxation timescales. However, the dynamics of $V_1(t)$ only under a reduced description, strictly speaking, is not Markovian. Both relaxation timescales of the full circuit may appear in its characteristics, in contrast to the behavior of an authentic single-RC circuit. This dynamical distinction is evidenced by the failure of FT. However, in the failed cases one can still observe a FT-like behavior, featuring a linear symmetry function with a non-unity slope.

In fig. 4 we present the autocorrelation and spectral density of our measured $V_1(t)$ for the small- (98.8 pF) and large-C_c (9.71 nF) cases, respectively, along with three theoretical expectations from ref. [15]. The solid line, which displays the theoretical expectation from the consideration of the full circuit, agrees very well with our experimental data in all cases. The dashed and dash-dotted lines represent theoretical expectations by a reduced circuit with descriptions (A) and (B), respectively. In the weak-coupling case (see figs. 4(a) and (b)), the expectations exhibit little difference, and the dynamics reveals a single relaxation only. Thus, the dynamics in the reduced descriptions is nearly Markovian, and FT remains valid for all τ. Under such regime, V_2 serves as a fast environment variable, which can be integrated as a part of the thermal background.

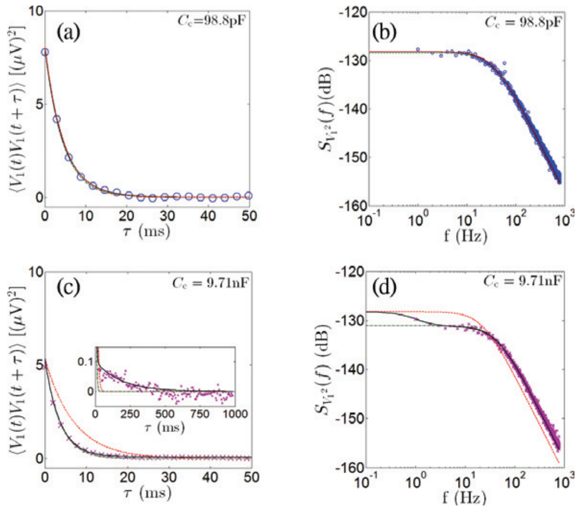

Fig. 4: (Colour online) Autocorrelation function and spectral density of $V_1(t)$. (a) Autocorrelation and (b) spectral density for $C_c = 98.8$ pF. (c) Autocorrelation and (d) spectral density for $C_c = 9.71$ nF. Experimental data are shown in symbols, and the solid, dashed, and dash-dotted lines represent theoretical predictions from the full description, reduced descriptions (A) and (B), respectively. The inset in (c) reveals a second exponential decay in the observed data at larger τ.

In the strong-coupling case (see figs. 4(c) and (d) for $C_c = 9.71$ nF), the measured noise level (shown by the plateau in fig. 4(d)) is seemingly reduced. Theoretically, the complete-description prediction reveals the existence of a second plateau at even smaller frequencies, while its noise level reaches the full magnitude. This implies a second, slow relaxation in V_1, which is evidenced remarkably by our experimental data in fig. 4(d). As a contrast, our reduced descriptions fail to depict the two-exponential relaxation. Nevertheless, the trace-out method (description (B)) succeeds in capturing the short-time, large-frequency relaxation precisely, while the naive description (description (A)) can faithfully represent the long-time, low-frequency result. As a result, FT of the entropy production holds for these two reduced descriptions only in the corresponding regimes where the reduced dynamics can be faithful. Note that the incorrect prediction of the entropy production $\langle\Delta\tilde{S}^{(\mathrm{B})}_{1\mathrm{tot},\tau}\rangle = \frac{I_1^2R_1}{T}\tau\left[1+\frac{R_1{C_c}^2}{R_2(C_2+C_c)^2}\right]$ in description (B) is also hinted by its failure to predict a real (smaller) noise level at low frequencies (see in fig. 4(d)).

The reduced effective noise in the masked circuit, as can be suggested from fig. 4(d), is caused by the correlation effect from the hidden variable V_2. In fact, in the regimes where FT fails, the linearity of symmetry functions suggests that it is possible to restore FT through the introduction of an effective noise strength. However, the effective noise strength can be dependent on the observation time τ. For example, in the small-τ limit, the effective noise strength is simply equal to that in description (B).

Moreover, in the large-τ regime, since the correlation effect diminishes, V_2 can be simply regarded as a part of thermal noises. The effective noise strength in such regime is equal to that of a single-RC circuit with resistance R_1 and thus coincides with that in description (A). We speculate that with the introduction of this effective noise strength, one can develop yet another reduced description which interpolates between descriptions (A) and (B), and FT can be valid in this reduced description for all values of τ.

As a comparison, in the system of ref. [3], FT has also been observed for small τ, and FT-like behavior was found for other ranges of τ. The apparent entropy production used in their work is in some sense similar to our description (B). Both approaches share the same spirit that the hidden degree of freedom is traced out from the probability distribution of the complete description. However, our effective dissipation function in description (B) is derived from the logarithm of the ratio of (traced-out) transition probabilities between forward and backward processes. On the other hand, the authors in ref. [3] started from the physical dissipation over the observed particle and estimated the force through the use of a "mean local velocity". The mathematical expressions derived from these two reduced descriptions are also distinct.

Conclusion. – In this work we use the argument of FT as a lever to open up an insight into the hidden-variable problem in statistical mechanics. In the reduced descriptions, we conclude that FT is approximately valid in the weak-coupling regime, where one can hardly differentiate between the two relaxation times of the system. Moreover, the failure of FT in the strong-coupling regime is itself a signature of non-Markovian dynamics. On the other hand, the observed FT-like behavior hints that even in the strong-coupling regime, this failure can be repaired through the redefinition of an effective noise strength. While our analysis is founded on the linearity of equations for the coupled network of RC circuits, the FT-like behavior has also been observed in the system of magnetically coupled particles [3] with a more complicated pairwise interaction. These observations lead us to the speculation that the heat-bath assumption, if properly adapted, can be considered in a broader range of studies.

* * *

This work has been supported by MOST 104-2112-M-008-009, 104-2112-M-008-003-MY3, and 103-2112-M-008-007-MY2. C-LL acknowledges the support from NCTS thematic group Complex Systems.

REFERENCES

[1] Crooks G. E., *Phys. Rev. E*, **60** (1999) 2721.
[2] Seifert U., *Rep. Prog. Phys.*, **75** (2012) 126001.
[3] Mehl J. *et al.*, *Phys. Rev. Lett.*, **108** (2012) 220601.
[4] Crisanti A., Puglisi A. and Villamaina D., *Phys. Rev. E*, **85** (2012) 061127.
[5] Kawaguchi K. and Nakayama Y., *Phys. Rev. E*, **88** (2013) 022147.
[6] Shiraishi N. and Sagawa T., *Phys. Rev. E*, **91** (2015) 012130.
[7] Nakayama Y. and Kawaguchi K., *Phys. Rev. E*, **91** (2015) 012115.
[8] Chun H. and Noh J. D., *Phys. Rev. E*, **91** (2015) 052128.
[9] Borrelli M. *et al.*, *Phys. Rev. E*, **91** (2015) 012145.
[10] van Zon R., Ciliberto S. and Cohen E. G. D., *Phys. Rev. Lett.*, **92** (2004) 130601.
[11] Garnier N. and Ciliberto S., *Phys. Rev. E*, **71** (2005) 060101(R).
[12] Joubaud S., Garnier N. and Ciliberto S., *EPL*, **82** (2008) 30007.
[13] Ciliberto S. *et al.*, *Phys. Rev. Lett.*, **110** (2013) 180601.
[14] Golubev D. S. and Pekola J. P., *Phys. Rev. B*, **92** (2015) 085412.
[15] Chiang K.-H., Chou C.-W., Lee C.-L., Lai P.-Y. and Chen Y.-F., arXiv:1601.04776 (2016).